A Wide Range and High Sensitivity four-channel Compact Electrochemical Biosensor for Neurotransmitter Detection on a Microfluidic Platform

Elnaz Ghodsevali[1, 2], Hamza Landari[1], Mounir Boukadoum[3], Benoit Gosselin[2], Amine Miled[1]
[1]LABioTRON Bioeng. Research Laboratory, ECE Dept. Laval University, Québec City, QC, Canada
[2] Biomedical Microsystems Laboratory, ECE Dept. Laval University, Québec City, QC, Canada
[3]Université du Québec à Montréal, QC, Canada
elnaz.ghodsevali.1@ulaval.ca; amine.miled@gel.ulaval.ca

***Abstract*— We present a four-channel, high-sensitivity and linearity electrochemical biosensor for neurotransmitter (NT) detection and measurement. Using a multi-channel microfluidic platform makes this biosensor capable of detecting NT-related currents going from nanoamperes to milliamperes, with a sensitivity of the order of picoamperes. Moreover, by using a fully differential potentiostat architecture, the biosensor offers a high common-mode rejection ratio (90 dB), making it appropriate for low-noise and high-sensitive applications. The system was implemented on a 15 mm x 15 mm PCB with direct interface to the microfluidic chambers. It was calibrated with a 5 mM ferrocyanide solution and successfully tested with dopamine at three concentrations. The system shows a minimum sensistivity of 100 pA and consumes 60 mW.**

I. INTRODUCTION

Over the past years, there have been many investigations of brain activity and neurological disorders. In this respect, understanding and detecting the dysfunctions of the electrochemical processes that occur within the nervous system can be of paramount importance. This is the case for brain signal propagation between cells, whose successful completion depends on mediating molecules at the neural synapses. These neurotransmitter (NTs) substances, known also as chemical messenger molecules, are the agents behind action potential propagation through the nervous system and knowing their presence and concentration is essential for understanding the gate-keeping role of synapses.

Electrochemical biosensing is a promising technology for detecting and quantifying NTs thanks to its high sensitivity, accuracy and selectivity, and also its portability [1]. The most common techniques use for Electrochemical biosensing are amperometry and voltammetry, in a typical setup, an excitation voltage is applied between a solution of the substance of interest and a reagent, and the redox current generated by the ensuing electrochemical reaction is measured. This current is proportional to the analyte's concentration. The potentiostat circuit is commonly used to perform the previous operations [2].

A potentiostat contains three main parts: a control unit, a measurement cell, and three electrodes with the cell named a working electrode (WE), reference electrode (RE) and counter electrode (CE). All three parts affect the performance of the system. During operation, a substance in solution is put in the measurement cell, and a voltage is applied across the WE and RE electrodes, while CE is used to inject a current to be measured over WE [5].

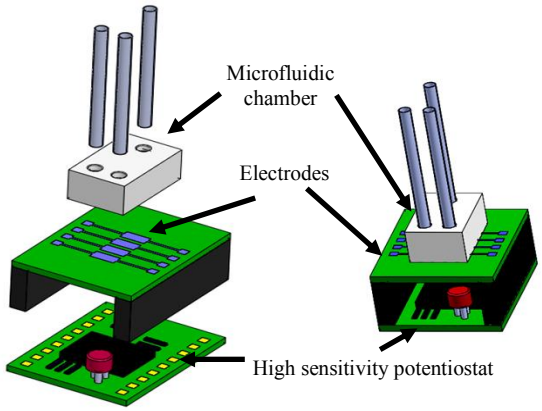

Fig. 1. System level diagram of the four-channel High-sensitivity-Potentiostat (HSP) architecture.

Every NT reacts at a specific cell voltage. Therefore, to detect many different NTs, it is necessary to have a wide input/output dynamic range circuit. To meet this constraint, a high density multi-channel microfluidic structure may be employed. Then, a major challenge to address in this microfluidic platform is dimension disparity between the electronic section of the biosensor and the microfluidic part [3, 4]. A fully differential (FD) potentiostat architecture must also be utilized [2, 6], since using the simpler single-ended (SE) amplifier-based architecture leads to insufficient input-output differential range when the supply voltage is decreased, with a subsequent reduction of the system's sensing range.

The system described in this work results from the hybrid integration of electronics and microfluidics parts for multi-channel sensing as shown in Fig.1. The objective of the design is to allow monitoring NT activity in small volume. Each sensor in the system has its own counter, reference and working electrodes, and a microfluidic structure sitting on top of the electronic part is designed in a Polydimethylsiloxane (PDMS) substrate to handle liquid flow between the in-channel electrodes. The four-channel FD potentiostat implemented in this work can detect a range of output currents from high picoamperes to low milliamperes.

978-1-4577-0220-4/16/$31.00 ©2016 IEEE

The paper is organized as follows: Section II provides background on the FD potentiostat and microfluidic platform; the proposed circuit is presented in section III and section IV provides our experimental results. Finally, section V concludes the paper.

II. BACKGROUND

A. FD Potentiostat

At the synaptic gap, several NTs are released, each with its own redox current value. Hence, detecting different molecules simultaneously mandates the need for a multichannel potentiostat. Each channel detects the molecules according to its applied voltage, V_{src}, such that:

$$V_{src} = V_{WE} - V_{RE} = V_{cell} \tag{1}$$

where V_{WE} and V_{RE} are the voltage at WE and RE, respectively and V_{cell} is the voltage across the considered solution. The generated redox current, I_{sense}, can be sensed through a resistor, R_{sense}, as shown in (2).

In order to be capable of quantifying various NTs with different I_{sense}, a wide range of input/output voltages should be covered by the channels, since:

$$V_{out} = I_{sense} R_{sense} \tag{2}$$

However, lowering the supply voltage for low power operation degrades the input/output voltage range, with a detrimental impact on the number of detectable molecules when using a single-ended potentiostat. The FD potentiostat mitigates this effect by maximizing the output voltage swing and dynamic range for a given supply voltage. The FD potentiostat also provides high sensitivity and accuracy due to high common-mode noise rejection, hence reducing noise interference at low sensed currents [2].

B. Microfluidic Structure

The microfluidic structure of the systems consists of a small 7.5 mm x 5 mm chamber with two inlets and one outlet. The chamber was designed with PDMS and it was bonded to a PCB with its bottom part was open and in direct contact with the WE, CE and REF electrodes designed on the PCB. An array of 4 x 10 electrodes was implemented inside the chamber as shown at Fig. 1. Each channel of the potentiostat is connected to each row and to only 3 electrodes in each row from the mentioned electrode array simultaneously. These three electrodes are CE, WE and RE. The dimension of the array was over estimated for ease of manipulation during the testing phase.

III. PROPOSED ARCHITECTURE

The schematic of one channel of the implemented FD potentiostat is shown in Fig. 2. Two buffers, OP1 and OP2, prevent the faradic current form leaking through the FD amplifier. Therefore, all this current is seen by sensing resistor R_{sense}, with the benefit of higher accuracy and linearity. An instrumentation amplifier with unity gain, OP3, is used at the output to convert the sensed current to voltage without danger of resistor mismatch between R_{sense} and the output stage. In Fig. 2, R_{ce} and R_{we} stand for the faradic

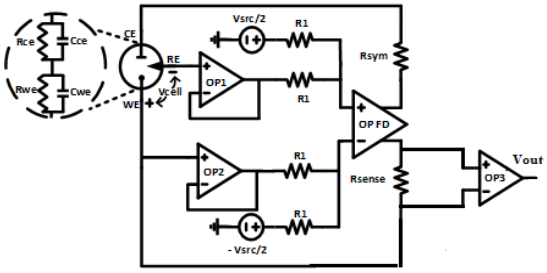

Fig. 2. Schematic of one channel of the implemented potentiostat; OP1 and OP2 are the buffers; OP3 is an instrumentation amplifier, and OP FD is a fully differential amplifier.

resistances and C_{ce} and C_{we} correspond to the double-layer capacitances related to CE and WE, respectively.

The output swing voltage of this FD potentiostat is approximately twice of a conventional SE one. It is given by [7]:

$$S_{FD} = 2|V_{dd} - V_{ss}| \frac{R_{we}}{R_{we} + R_{sense} + R_{sym} + R_{ce}} \tag{3}$$

where R_{sym} keep the symmetric operation in the feedback loop according to existence of R_{sense}.

As mentioned before, noise has an important effect on the sensitivity of the potentiostat. The signal-to-noise (SNR) of this circuit is [6, 7]:

$$SNR = \frac{(I_{sense} R_{sense})^2}{i_{op3}^2 R_{sense}^2 + V_{op3}^2 + V_{R_{sense}}^2} \tag{4}$$

where i_{op3}^2 and V_{op3}^2 stand for the equivalent mean-squared input current noise and the equivalent mean-squared input voltage noises of OP_3, respectively and V_{Rsense}^2 is the equivalent mean-squared noise of R_{sense}. From (4), it is obvious that R_{sense} is the main contributor to SNR as it contributes to both signal and noise [7]. Therefore, while configuring the potentiostat with a higher R_{sens} makes it benefit from low current sensing as (2) shows, it will come at the expense of having influence on the generated noise. In other words, higher R_{sense} values allow for lower current sensing, but with degraded accuracy. In the proposed system, four values of R_{sense}, 1KΩ, 10KΩ, 100KΩ and 1MΩ were used for each micro-channel to make the described biosensor capable of quantifying a wide range of sensing currents. By means of this technique, more NTs with different concentration could be quantified.

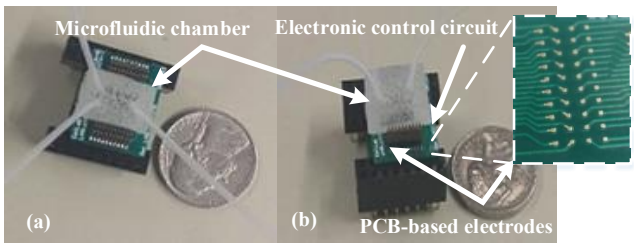

Fig. 3. Implemented potentiostat with microfluidics system (a) top-view (b) side-view.

IV. Experimental Results

The implemented system is shown in Fig. 3, where we see the discrete potentiostat and the microfluidic structure sitting on top of the electrodes. A dual low noise amplifier, LMC662 from Texas Instruments (USA), was used for OP_1 and OP_2 to improve overall SNR. An instrumentation amplifier with low bias current and noise, INA121, suitable for biosensor applications buffers R_{sense} and converts its current to voltage. OP-FD, THS4541, is a rail-to-rail FD amplifier with 100 dB CMRR to improve the common-mode noise rejection of the circuit and therefore the detection of low concentration analytes. The system was tested with ferrocyanide for one hour continuously. Obtained results were almost identical which proves that the reaction was approximately reversible.

Fig. 4 illustrates the functionality of the implemented system via the electrochemical analysis of a 5 mM ferrocyanide solution using gold coated RE, WE and CE electrodes. This plot shows the CV of ferrocyanide for R_{sense}=100 KΩ and given the different scan rates indicated. The increment in both reduction and oxidation peaks form 7 µA and -7 µA to 17 µA and -13 µA, respectively, is shown for a scan rate going from 80 mV/s to 640 mV/s.

The minimum detectable redox current of different ferrocyanide solutions at each of the four channels is illustrated in the CV plots shown in Fig. 5.a and 5.b. In Fig. 5.a, the sensitivity when using R_{sense}= 1 KΩ and R_{sense}= 10 KΩ was 3.08 µA and 1.98 µA, respectively. In Fig. 5.b, the sensitivity for minimum detectable concentration of ferrocyanide through the channels with R_{sense} of 100 KΩ and 1 MΩ, was 610 nA and 101 nA, respectively. Fig. 6 plots the circuit sensitivity calibration for different channels. It shows a high linearity as the regression factor was 0.9723.

Fig. 7 shows the biosensor responses for a dopamine solution (Sigma Aldrich) with concentrations of 1 mM, 100 µM to 10 µM, and R_{sense} set to 10 KΩ, 100 KΩ and 1 MΩ, respectively. As the figure shows, sensitivity of the system is higher for the channels with higher R_{sense} values.

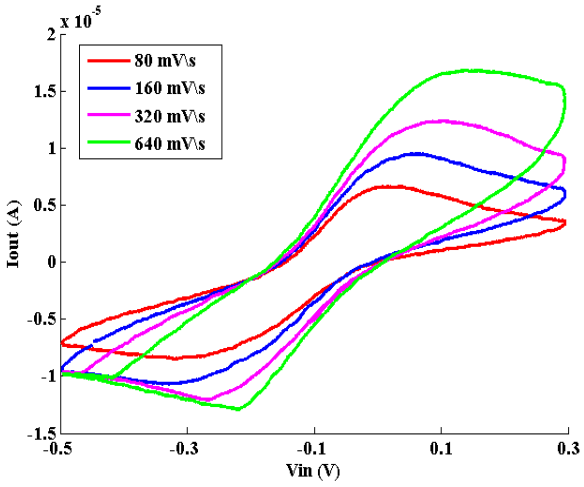

Fig. 4. CV of 5 mM Ferricyanide over different scan rates with R_{sense} = 100 KΩ.

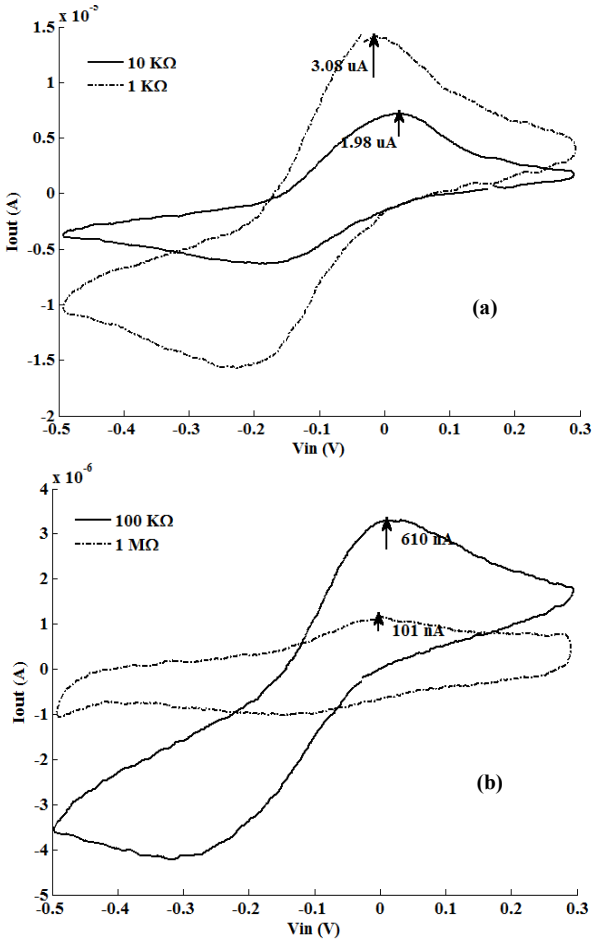

Fig. 5. Output sensed current of minimum detectable concentrations of Ferrocyanide through the channels for: (a) R_{sense}=1 KΩ and R_{sense}=10 KΩ (b) R_{sense}=100 KΩ and R_{sense}=1 MΩ.

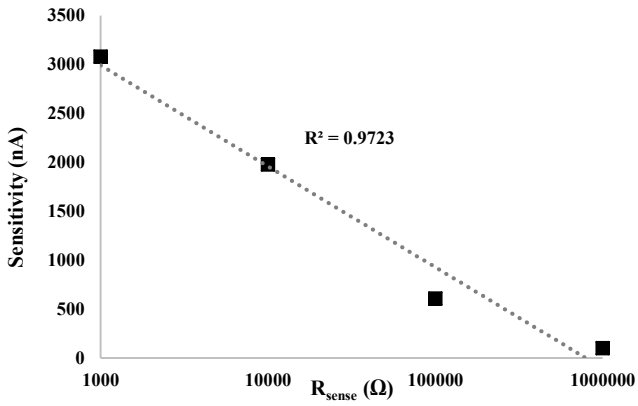

Fig. 6. Sensitivity calibration of the system tested with Ferrocyanide.

Fig. 8 shows the output noise voltage, V_{rms}. It is seen from this figure that the reduction of noise with increasing of the R_{sense} is not linear. Indeed, by increasing the R_{sense} the degradation in V_{rms} is lowered. Hence, the sensitivity improves linearly with R_{sense} and V_{rms} decreases logarithmic. Consequently, SNR is more affected by the noise when using higher R_{sense}. In other words, SNR is not increasing linearly with increment of R_{sense}, however; the sensitivity is increasing linearly.

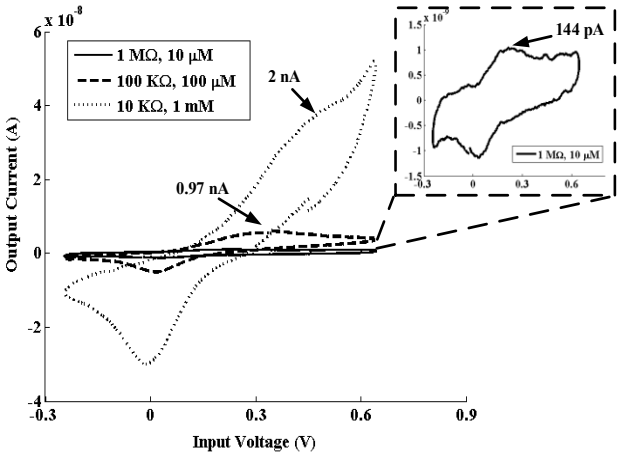

Fig. 7. Output sensed current at minimum detectable concentrations of dopamine through a channel for indicated R_{sense} and dopamine concentration values.

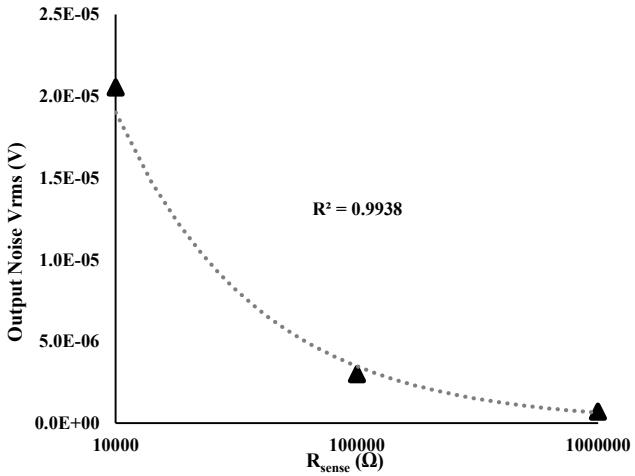

Fig. 8. Output Noise Vrms over different R_{sense} for dopamine analysis.

The results of our system in comparison to other works are provided in Table 1. As can be seen, this design offers a higher dynamic range of output voltage and covers a wider sensitivity range. On the other hand, the supply voltage and power consumption are higher. We are working on an integrated lab-on-chip version to address this issue.

TABLE 1. SUMMARY OF CHARACTERIZATIONS OF PROPOSED SYSTEM.

Parameters	This Work	[2]	[8]
Power Supply	**5 V**	3.3 V	1.8 V
Power consumption	**60 mW**	60 μW	72.36 μW
Dynamic range Vout	**76 dB**	70 dB	33.97 dB
Sensitivity range	**100 pA-10 μA**	100p-60nA	100nA-5μA
R^2 of system linearity	**0.9723**	N.A	N.A
CMRR	**90 dB**	N.A	N.A
Implemented circuit type	**Fully Differential four channel**	Fully Differential	Differential difference

N.A = Not Applicable

V. CONCLUSION

In this paper, we presented a four-channel FD potentiostat architecture for NT measurement. The proposed design is able to measure a wide range of analyte concentrations, with its redox current sensitivity from picoamperes to milliamperes thanks to different R_{sense} for each channel. The system presented a sensitivity of approximately 100 pA for R_{sense} = 1 MΩ. In addition, this potentiostat showed a linear behavior through different channels while consuming 60 mW of power at 5v supply.

ACKNOWLEDGMENT

The authors acknowledge the financial support from the National Research Council of Canada (NSERC). The Microsystems Strategic Alliance of Québec (ReSMIQ).

REFERENCES

[1] M. Poustinchi, R. G. Stacey, S. Musallam, "Implantable Microsystem for Concurrent Measurement of Brain's Action Potential and Neurotransmitter," in Proc. Medical Measurements and Applications (MeMeA), Jun 2014.

[2] M. Nazari and R. Genov, "A fully differential CMOS potentiostat," in Proc. IEEE Int. Symp. Circuits and Systems (ISCAS), May 2009.

[3] Y. Huang, A. J. Mason, "Lab-on-CMOS Integration of Microfluidics and Electrochemical Sensors," Lab Chip, vol. 13, pp. 3929–3934, 2013.

[4] M. Vergani, ,G. Ferrari, M. Sampietro, L. Amato, A. Heiskanen, M. Dimaki, W. E. Svendsen, J. Emnéus, "Compact Potentiostat for Cellular Electrochemical Imaging with 54 Parallel Channels," in Proc. IEEE Biomedical Circuits and Systems Conference (BioCAS), Nov 2012.

[5] M. M. Ahmadi, G. A. Jullien, "A Very Low Power CMOS Potentiostat for Bioimplantable Applications," in Proc.System-on-Chip for Real-Time Applications, July 2005.

[6] S. Martin , F. Gebara , T. Strong and R. Brown, "A fully differential potentiostat," IEEE Sensors Journal, vol. 9,pp. 135-142, 2009.

[7] E. Ghodsevali, B. Gosselin, M. Boukadoum, A. Miled, "High Accuracy and Sensitivity Differential Potentiostat with Amplifier-Based Error Cancellation Feedback Loop," in Proc. IEEE Biomedical Circuits and Systems Conference (BioCAS), Oct 2015.

[8] K. A. A. Mamun, N. McFarlane, "A CMOS potentiostatic glucose monitoring system for VACNF amperometric biosensors," in Proc. IEEE Int. Symp. Circuits and Systems (ISCAS), May 2015.